

Supplementary Information

Orientational Analysis of R134a–R134a Interactions in the First Solvation Shell

Figure S1 shows the distribution of the angle between the CC vector and the intermolecular vector CoCC–CoCC of pairs of R134a molecules at 272 K and 11.55 bar. A large peak appears at about 5.0 Å and about 90° and two small peaks are located at a CoCC–CoCC distance of about 5.2 Å and angles of 0° and 180°. This distribution gives us the spatial distribution of neighbouring R134a molecules around a central molecule. Based on this observation, the neighbouring molecules prefer to locate on a circle of radius 5.0 Å around the midpoint of the CC bond of the central R134a molecule. They also have a preference to be in the space above and below the central molecule. This is also observed in pure R134a.¹ Next, we shall investigate the orientation of the neighbouring molecules in each of these spaces.

The space around the central molecule is divided into four sections: π_F , π_H , π_T and π_B as in our previous study¹ (Figure S2). We use a plane that cuts through C2C3 and is perpendicular to the C2C3F6 plane to separate the spaces π_F and π_H . Figure S3a shows the distribution of the angle between C2C3 vectors at different CoCC–CoCC distances in the space π_F . The C2C3 vectors of the nearest neighbours in this space of the first solvation shell prefer a perpendicular alignment. However, other angles of C2C3 vectors close to 90° are also preferred. Figure S3b shows the distribution of the angle between R134a dipoles. A peak appears at 0°; thus, the dipole moments have a preference for a parallel alignment. Figure S3c depicts the preferred orientations of the neighbouring molecules in the π_F space of the first solvation shell.

Figure S4a shows the distribution of the angle between C2C3 vectors at different CoCC–CoCC distances in the space π_H . At a CoCC–CoCC distance of 5.0 Å, vectors C2C3 of the nearest neighbours in the first solvation shell prefer to make an angle of about 90° with each other. However, this peak is quite broad tailing towards 0° and therefore other angles smaller than 90° are also populated. At a CoCC–CoCC distance of about 4.7 Å, a small peak at 180° is observed, which suggests that, at short distances, the C2C3 vectors have a preference for antiparallel alignment. This alignment of the angle between C2C3 vectors is not observed in the π_F space. The distribution of the angle of dipoles of R134a molecules is shown in Figure S4b. A peak at 0° is observed, which indicates that the dipole moments have a strong preference for a parallel alignment. This was also observed in the π_F space. Figure S4c shows an example of the alignment of a pair of R134a molecules in the π_H space of the first solvation shell.

To analyse the preferred orientations of the neighbouring molecules sitting above (and below) the central molecule in the first solvation shell, we use the same distribution of the angles as for the analysis of π_F and π_H spaces. Figure S5a shows that at about 5.2 Å, the C2C3 vectors of the nearest neighbouring molecules prefer a parallel alignment, as a sharp peak is observed at 0°. The distribution of the average angle between dipoles (Figure S5b) also reveals that the dipoles prefer to be parallel to each other. Figure S5c illustrates the preferred orientation of neighbours sitting on top of the central molecule. A similar orientation is preferred by the molecule that sits at the bottom of the central molecule in the first solvation shell (Figure S6). To this end, we can conclude that the orientational distribution of the neighbouring R134a molecules around the central R134a molecule at 272 K and 11.55 bar is the same as that in pure R134a liquid¹, which agrees

with the RDFs study. The ODFs again confirm that the presence of CO₂ in the liquid mixture R134a + CO₂ does not alter the structure of R134a.

Reference

1. H. Do, R. J. Wheatley and J. D. Hirst, *Phys. Chem. Chem. Phys.*, 2010, **12**, 13266–13272.

Table S1: Thermodynamic properties of the binary mixture R134a + CO₂ at 252 K

P (bar)	ρ_L (kg/m ³)	ρ_V (kg/m ³)	U_L (kJ/mol)	U_V (kJ/mol)	x_A	y_A
3.010	1340.6 (5.3)	11.44 (0.4)	-9.22 (0.1)	10.58 (0.1)	0.095 (0.005)	0.480 (0.007)
5.080	1313.7 (7.5)	15.83 (0.4)	-8.33 (0.1)	10.49 (0.1)	0.225 (0.006)	0.713 (0.005)
6.830	1294.9 (6.9)	19.53 (0.7)	-7.17 (0.2)	10.46 (0.1)	0.322 (0.008)	0.808 (0.003)
8.000	1263.3 (10)	21.77 (0.9)	-6.72 (0.2)	10.43 (0.1)	0.418 (0.004)	0.861 (0.006)
10.03	1240.5 (11)	26.56 (1.3)	-5.47 (0.3)	10.33 (0.1)	0.521 (0.005)	0.901 (0.012)
12.02	1203.8 (11)	32.03 (1.9)	-4.63 (0.2)	10.30 (0.1)	0.628 (0.009)	0.924 (0.008)
13.57	1150.9 (11)	35.32 (2.5)	-3.63 (0.2)	10.31 (0.1)	0.750 (0.010)	0.946 (0.009)
15.76	1109.3 (12)	41.17 (2.2)	-2.57 (0.2)	9.888 (0.1)	0.857 (0.013)	0.970 (0.010)
16.85	1086.5 (11)	42.39 (2.2)	-2.55 (0.2)	9.860 (0.1)	0.894 (0.011)	0.984 (0.008)

* P : saturated pressure, ρ : density, U : configurational potential energy, x_A : mole fraction of CO₂ in the liquid phase, y_A : mole fraction of CO₂ in the vapour phase, the numbers in parentheses indicate the uncertainties at 95% confidence level.

Table S2: Thermodynamic properties of the binary mixture R134a + CO₂ at 272 K

P (bar)	ρ_L (kg/m ³)	ρ_V (kg/m ³)	U_L (kJ/mol)	U_V (kJ/mol)	x_A	y_A
3.940	1292.6 (5.5)	17.35 (0.4)	-7.44 (0.1)	11.29 (0.1)	0.034 (0.004)	0.196 (0.008)
5.340	1284.4 (7.3)	20.74 (0.8)	-6.99 (0.2)	11.27 (0.1)	0.081 (0.005)	0.387 (0.006)
6.440	1274.8 (12)	23.91 (0.7)	-6.54 (0.3)	11.16 (0.1)	0.121 (0.007)	0.466 (0.004)
6.980	1266.5 (7.7)	24.52 (0.9)	-6.52 (0.2)	11.15 (0.1)	0.144 (0.005)	0.536 (0.005)
8.620	1251.3 (11)	27.24 (1.2)	-5.86 (0.3)	11.13 (0.1)	0.210 (0.006)	0.643 (0.011)
9.770	1241.6 (7.2)	30.25 (0.9)	-5.78 (0.2)	11.12 (0.1)	0.261 (0.008)	0.700 (0.007)
11.55	1223.6 (7.2)	34.82 (1.4)	-5.66 (0.2)	11.10 (0.1)	0.320 (0.009)	0.741 (0.006)
14.54	1196.6 (8.6)	42.31 (1.8)	-4.63 (0.2)	11.03 (0.1)	0.432 (0.012)	0.808 (0.011)
16.07	1170.7 (11)	42.92 (1.5)	-3.93 (0.3)	11.00 (0.1)	0.501 (0.012)	0.864 (0.009)
18.21	1164.5 (12)	49.51 (2.8)	-3.20 (0.2)	10.79 (0.1)	0.533 (0.011)	0.868 (0.011)
20.33	1107.2 (12)	53.53 (2.6)	-1.95 (0.1)	10.75 (0.1)	0.667 (0.013)	0.911 (0.012)

* P : saturated pressure, ρ : density, U : configurational potential energy, x_A : mole fraction of CO₂ in the liquid phase, y_A : mole fraction of CO₂ in the vapour phase, the numbers in parentheses indicate the uncertainties at 95% confidence level.

Table S3: Thermodynamic properties of the binary mixture R134a + CO₂ at 292 K

P (bar)	ρ_L (kg/m ³)	ρ_V (kg/m ³)	U_L (kJ/mol)	U_V (kJ/mol)	x_A	y_A
8.230	1215.9 (6.2)	34.61 (1.1)	-4.85 (0.1)	11.82 (0.1)	0.054 (0.006)	0.240 (0.006)
9.320	1202.0 (4.9)	37.31 (1.2)	-4.63 (0.1)	11.80 (0.1)	0.087 (0.004)	0.338 (0.007)
11.27	1204.7 (9.9)	42.42 (1.4)	-3.99 (0.2)	11.67 (0.2)	0.124 (0.007)	0.443 (0.005)
13.97	1187.1 (9.1)	50.79 (2.2)	-3.93 (0.1)	11.66 (0.2)	0.183 (0.005)	0.552 (0.007)
17.16	1160.2 (12)	53.94 (2.3)	-3.46 (0.3)	11.62 (0.2)	0.289 (0.007)	0.668 (0.010)
19.16	1156.1 (13)	64.67 (2.4)	-2.96 (0.3)	11.51 (0.2)	0.305 (0.008)	0.692 (0.012)
20.48	1138.1 (11)	62.53 (2.7)	-2.90 (0.2)	11.49 (0.2)	0.362 (0.011)	0.726 (0.011)

* P : saturated pressure, ρ : density, U : configurational potential energy, x_A : mole fraction of CO₂ in the liquid phase, y_A : mole fraction of CO₂ in the vapour phase, the numbers in parentheses indicate the uncertainties at 95% confidence level.

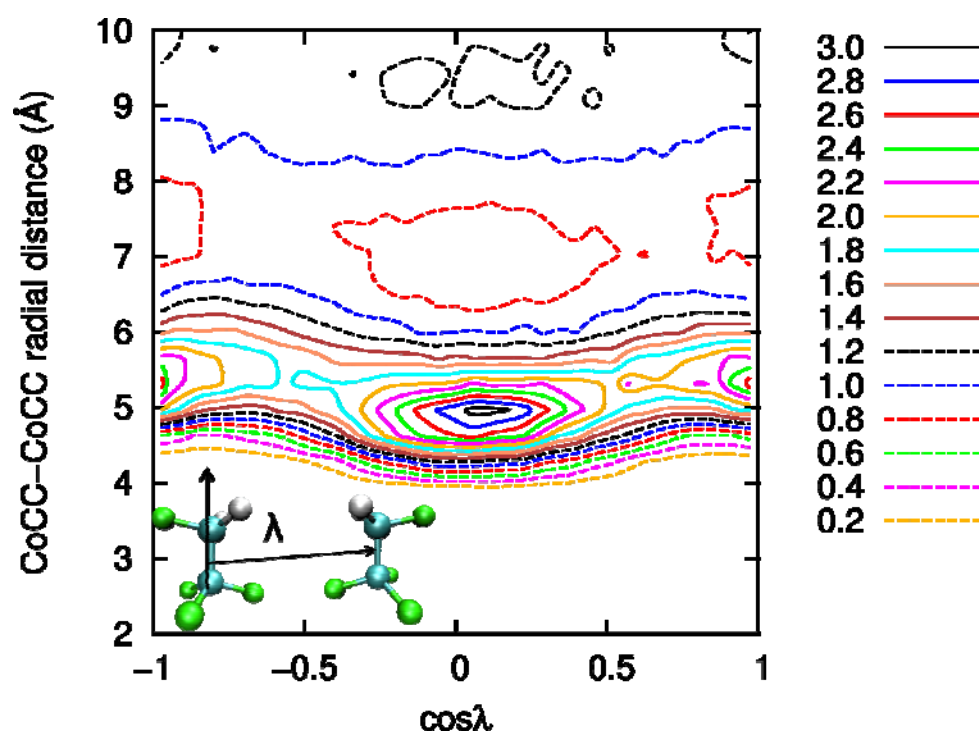


Figure S1. Distribution of the angle between C2C3 vector and CoCC-CoCC vector in R134a + CO₂ liquid mixture at 272 K and 11 bar.

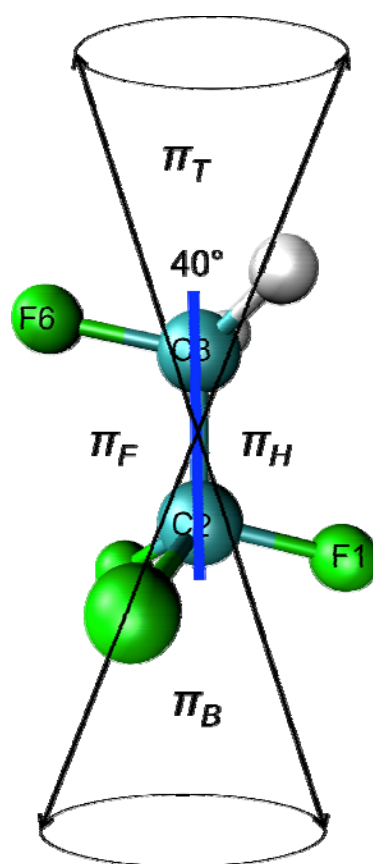


Figure S2. Schematic of the division of the space around the reference molecule. π_F is the space that contains the fluorine atom of the CH_2F group, π_H is the space that contains the hydrogen atoms of the CH_2F group, π_T is the space above the reference molecule, and π_B is the space below the reference molecule.

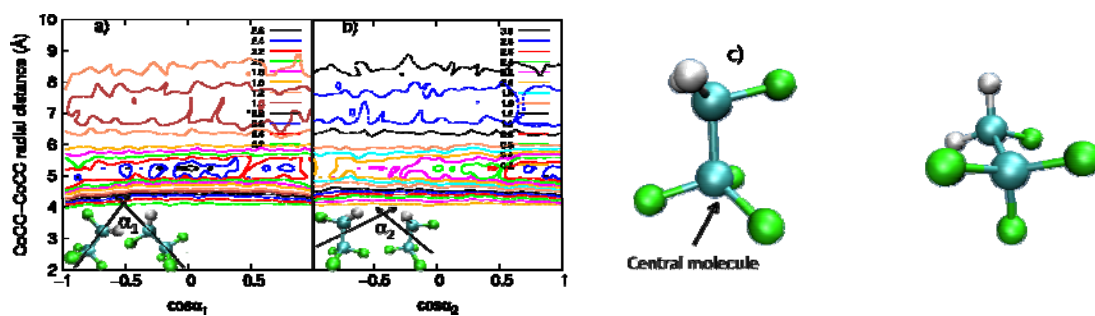


Figure S3. Distribution of (a) the angle between C2C3 vectors (α_1), (b) the angle between dipole vectors (α_2), and the nearest neighbour interaction (c) in π_F space in R134a + CO₂ liquid mixture at 272 K and 11 bar.

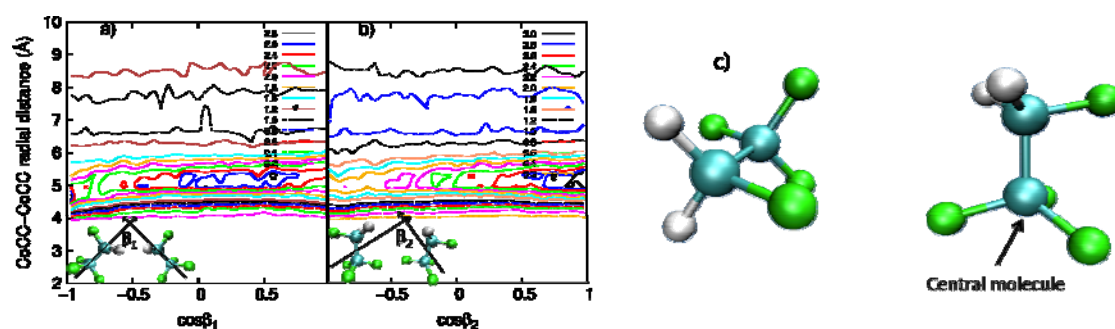


Figure S4. Distribution of (a) the angle between C2C3 vectors (β_1), (b) the angle between dipole vectors (β_2), and the nearest neighbour interaction (c) in π_H space in R134a + CO₂ liquid mixture at 272 K and 11 bar.

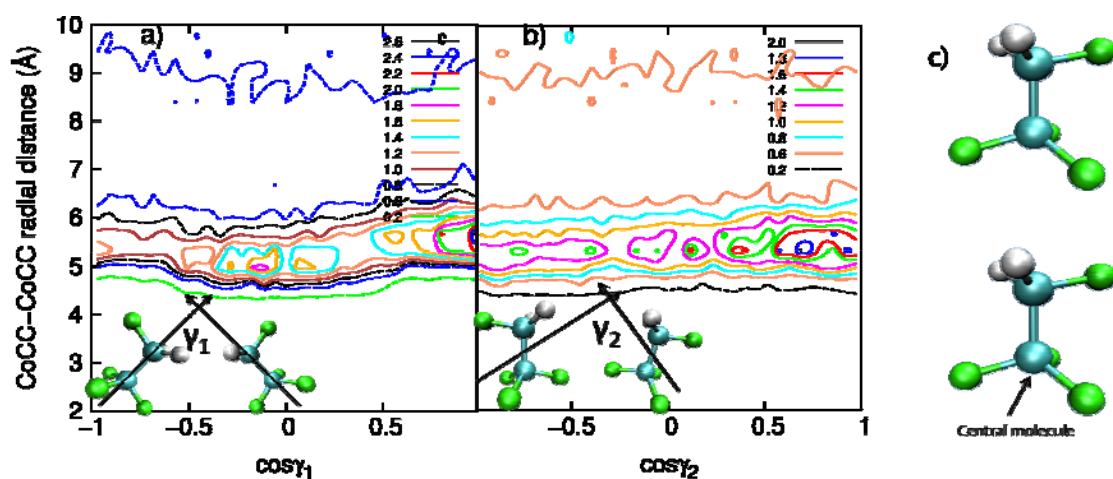


Figure S5. Distribution of (a) the angle between C2C3 vectors (γ_1), (b) the angle between dipole vectors (γ_2), and the nearest neighbour interaction (c) in π_T space in R134a + CO₂ liquid mixture at 272 K and 11 bar.

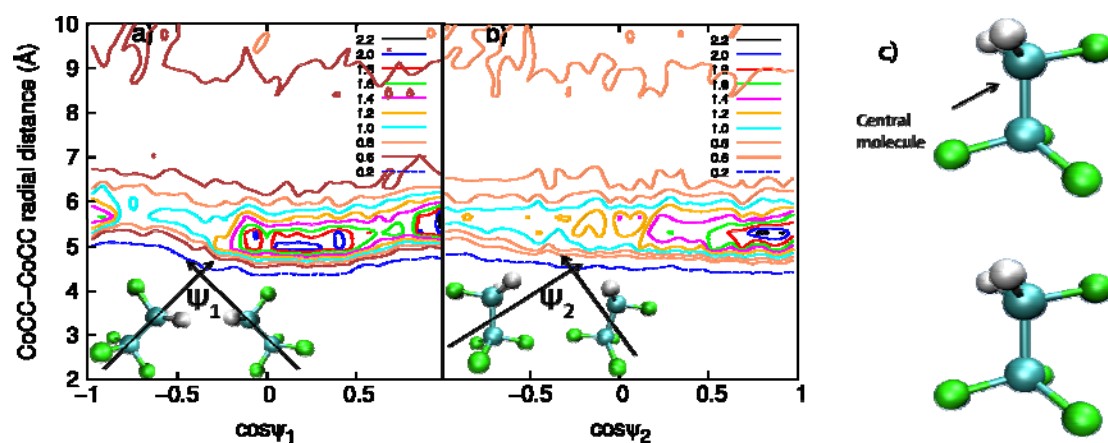


Figure S6. Distribution of (a) the angle between C2C3 vectors (ψ_1), (b) the angle between dipole vectors (ψ_2), and the nearest neighbour interaction (c) in π_B space in R134a + CO₂ liquid mixture at 272 K and 11 bar.